

**Bronzes with a Tunnel Structure  $\text{Rb}_x\text{P}_8\text{W}_{8n}\text{O}_{24n+16}$**   
**II. The Third Term of the Series:  $\text{Rb}_x\text{P}_8\text{W}_{24}\text{O}_{88}$**

BY J. P. GIROULT, M. GOREAUD, PH. LABBÉ AND B. RAVEAU

*Laboratoire de Cristallographie et Chimie du Solide, LA 251, Institut des Sciences de la Matière et du Rayonnement, Université de Caen, 14032 Caen CEDEX, France*

(Received 3 November 1980; accepted 6 December 1980)

### Abstract

The structure of  $\text{Rb}_x\text{P}_8\text{W}_{24}\text{O}_{88}$ , term  $n = 3$  of the series  $\text{Rb}_x\text{P}_8\text{W}_{8n}\text{O}_{24n+16}$ , has been solved by X-ray analysis. The solution in the mean cell of symmetry  $P2/m$  with  $a = 13.991$  (3),  $b = 3.7650$  (5),  $c = 8.561$  (1) Å,  $\beta = 114.22$  (1)° has led to  $R = 0.039$  and  $R_w = 0.044$  for 820 measured reflections with  $\sigma(I)/I \leq 0.333$ . The splitting of several O atoms involves the tilting of some  $\text{WO}_6$  octahedra. It results in a doubling of the  $b$  and  $c$  parameters, which has been confirmed by electron microscopy. The actual structure has thus been described with the true cell  $a$ ,  $2b$ ,  $2c$ , space group  $A2/m$ . A comparison is made with the term  $n = 4$  of the series, especially about the behaviour of the  $\text{P}_2\text{O}_7$  groups and the  $\text{WO}_6$  octahedra.

### Introduction

The study of the oxide  $\text{Rb}_x\text{P}_8\text{W}_{32}\text{O}_{112}$  (Giroult, Goreaud, Labbé & Raveau, 1980) has shown the capability of the tetrahedral groups  $\text{P}_2\text{O}_7$  to accommodate the octahedral framework of the perovskite. The possibility of existence of a series of microphases  $\text{Rb}_x\text{P}_8\text{W}_{8n}\text{O}_{24n+16}$  related to this structure, the only modification being the width of the perovskite slabs, was thus considered. The present paper deals with the third term of the series, for which a single-crystal study allows a comparison with the term  $n = 4$  previously described.

### Experimental

#### Sample preparation

Mixtures of  $\text{H}(\text{NH}_4)_2\text{PO}_4$ ,  $\text{Rb}_2\text{CO}_3$  and  $\text{WO}_3$  in appropriate ratios were first heated in air at 900 K to decompose the phosphate and carbonate. After addition of the theoretical amount of tungsten to obtain the composition  $\text{Rb}_x\text{P}_8\text{W}_{24}\text{O}_{88}$ , the samples were heated for eight days at 1250 K in a platinum crucible

placed in an evacuated silica ampoule. Crystals were selected from the preparation of nominal composition  $\text{Rb}_{1.6}\text{P}_8\text{W}_{24}\text{O}_{88}$ . The corresponding diffraction powder pattern was indexed in the mean cell:  $a = 13.994$  (2),  $b = 3.765$  (1),  $c = 8.564$  (2) Å,  $\beta = 114.24$  (1)°.

#### Determination of the mean structure

Tests with large samples generally showed crystals of poor quality. The crystal selected for the structure determination was small with dimensions  $12 \times 18 \times 96$  µm. Since its morphology was ill defined, absorption corrections were not applied. The monoclinic cell parameters, measured on Weissenberg films, were confirmed by diffractometric techniques with a least-squares refinement based on 25 reflections:  $a = 13.991$  (3),  $b = 3.7650$  (5),  $c = 8.561$  (1) Å,  $\beta = 114.22$  (1)°. No systematic absences occurred, suggesting the space groups  $P2/m$ ,  $P2$  or  $Pm$ . At this stage of the study, no superstructure reflections involving the doubling of  $b$  or  $c$  were observed.

The data were collected on a CAD-4 Enraf–Nonius diffractometer with  $\text{Mo } K\alpha$  radiation and a graphite monochromator. The intensities were measured up to  $2\theta = 88^\circ$  by the  $\omega$ - $2\theta$  technique with a maximum scan width of  $1.35^\circ$  and a counter slit aperture of 3.70 mm. The background intensity was measured on both sides of each reflection. A periodic control verified the stability of the sample. Among the 2887 independent measured reflections, 820 which had  $\sigma(I)/I \leq 0.333$  were corrected for Lorentz and polarization effects. The structure was solved by the heavy-atom method in  $P2/m$ . The W atom positions were fixed by the Patterson function and refined by least squares. The other atoms were located in the subsequent difference synthesis. The maps of electron density, studied for Rb, P and each independent O atom, showed a partial occupation of the corresponding sites, particularly 50% for P and the O atoms except O(2), O(4) and O(11). The occupation of Rb was determined by the later refinement at 45.6%. The electron density for Rb and P is almost spherical whereas a splitting is evident for O atoms. So it appears that the O atoms around the Rb

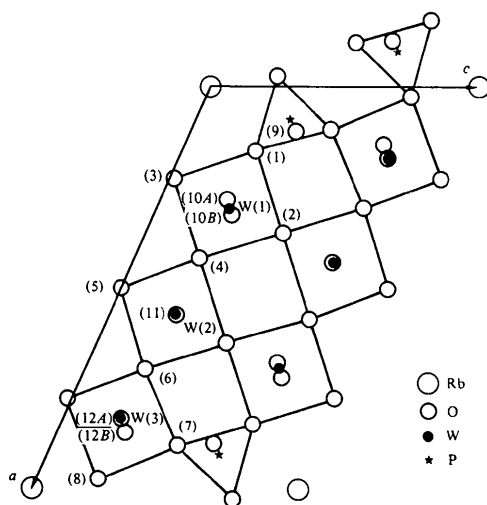


Fig. 1. Projection of the mean structure on to (010).

and P sites are distributed over two neighbouring positions as for  $\text{Rb}_x\text{P}_8\text{W}_{32}\text{O}_{112}$ , further O atoms being undisturbed. With the split positions introduced, the coordinates of all the atoms were then refined by full-matrix least squares. Scattering factors for  $\text{W}^{6+}$ ,  $\text{Rb}^+$ , and P were from Cromer & Waber (1965) corrected for anomalous dispersion (Cromer, 1965) and for  $\text{O}^{2-}$  from Suzuki (1960). A linear weighting scheme was adjusted according to  $\langle w|F_o| - |F_c| \rangle$  in terms of  $\sin \theta/\lambda$ . The refinement with anisotropic thermal coefficients for W and Rb atoms led to  $R = \sum ||F_o| - |F_c|| / \sum |F_o| = 0.039$  and  $R_w = |\sum w(|F_o| - |F_c|)^2 / \sum w|F_o|^2|^{1/2} = 0.044$ . Final atomic parameters for the mean cell of content  $\text{Rb}_{0.45}\text{P}_2\text{W}_6\text{O}_{22}$  are given in Table 1 and the corresponding projection on to (010) is shown in Fig. 1.\*

### The actual structure

In the mean cell, the same observations as in the term  $n = 4$  of the series  $\text{Rb}_x\text{P}_8\text{W}_{8n}\text{O}_{24n+16}$  can be made: partial occupancy of Rb and P sites, too short P-P distances (0.67 Å), splitting of O atoms. In a first step, a doubling of  $b$  and the tilting of the  $\text{W}(1)\text{O}_6$  and  $\text{W}(3)\text{O}_6$  octahedra can thus be considered. Then a projection of one sheet on to (010) can be drawn starting from a  $\text{PO}_4$  tetrahedron (Fig. 2). The tilting of the octahedra is indeed well defined, but the period of 8.56 Å along the [001] direction disappears because two  $\text{WO}_6$  octahedra which are  $c$  apart are tilted in an opposite manner. Then, the doubling of  $c$  is necessary and the actual cell, imposed by the tilting, is  $a, 2b, 2c$ .

\* Lists of structure factors and anisotropic thermal parameters have been deposited with the British Library Lending Division as Supplementary Publication No. SUP 35992 (7 pp.). Copies may be obtained through The Executive Secretary, International Union of Crystallography, 5 Abbey Square, Chester CH1 2HU, England.

Table 1.  $\text{Rb}_{0.45}\text{P}_2\text{W}_6\text{O}_{22}$ : positional parameters and e.s.d.'s in the mean cell  $a, b, c$ , space group  $P2/m$

$B_{\text{eq}}$  is defined as  $\frac{1}{3} \sum_i \sum_j \beta_{ij} a_i \cdot a_j$ .

Occupation	x	y	z	$B$ (Å <sup>2</sup> )
Rb	0.45 (3)	0	0	$B_{\text{eq}} = 1.62$ (29)
P	0.50	0.0839 (7)	0.5885 (27)	0.36 (11)
W(1)	1	0.30461 (11)	↓	$B_{\text{eq}} = 0.34$ (12)
W(2)	1	0.56167 (16)	↓	$B_{\text{eq}} = 0.31$ (8)
W(3)	1	0.82200 (10)	↓	$B_{\text{eq}} = 0.64$ (4)
O(1)	0.50	0.1612 (22)	0.438 (10)	0.04 (41)
O(2)	1	0.3644 (17)	↓	0.36 (22)
O(3)	0.50	0.2265 (23)	0.451 (12)	0.28 (46)
O(4)	1	0.4249 (15)	↓	0.45 (26)
O(5)	0.50	↓	0.442 (26)	1.0 (1.0)
O(6)	0.50	0.6998 (22)	0.444 (16)	0.67 (63)
O(7)	0.50	0.8925 (22)	0.585 (10)	0.75 (42)
O(8)	0.50	0.9781 (23)	0.463 (15)	0.95 (55)
O(9)	0.50	0.1091 (32)	0	0.66 (56)
O(10A)	0.50	0.2796 (36)	0	0.2501 (69)
O(10B)	0.50	0.3179 (37)	0	0.90 (55)
O(11)	1	0.5658 (24)	0	0.69 (28)
O(12A)	0.50	0.8243 (47)	0	0.98 (87)
O(12B)	0.50	0.8599 (42)	0	0.79 (77)

An electron microscopy study gives unambiguously the parameters  $a, 2b, 2c$ . The only observed reflections ( $hkl, k + l = 2n$ ) agree with the space group  $A2/m$  which is involved in the projection of Fig. 2. With the notation  $A2/m$  chosen here, the  $c$  axes are identical in both structures  $n = 3$  and  $n = 4$ , allowing their comparison. Here, the  $a$  axis does not have the same orientation as in the term  $n = 4$ , because the suppression of a row of  $\text{WO}_6$  octahedra in the perovskite slab of this compound involves a lack of periodicity at a short distance in the original direction. Atomic positions in the actual cell are given in Table 2, where the occupation is 1 for all atoms except Rb (0.91). With this hypothesis, a structure factor calculation for all the superstructure reflections was made, and it appeared that, as for the term  $n = 4$  of the series, only a few reflections corresponded to a measurable intensity. The strongest was about 1% of the maximum intensity of the whole spectrum. To confirm the

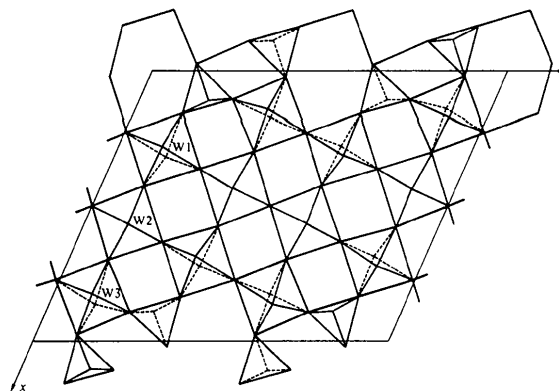


Fig. 2. Projection of the actual structure on to (010) limited to the oxygen framework from  $y = 0$  to  $y = 0.5$ .

Table 2.  $\text{Rb}_{1-82}\text{P}_8\text{W}_{24}\text{O}_{88}$ : positional parameters in the actual cell  $a, 2b, 2c$ , space group  $A2/m$ 

	x	y	z
Rb	0	0	0
P	0.0839	0.2942	0.1763
W(1)	0.30461	$\frac{1}{4}$	0.13896
W(2)	0.56167	$\frac{1}{4}$	0.12050
W(3)	0.82200	$\frac{1}{4}$	0.10463
O(1)	0.1612	0.2191	0.1392
O(2)	0.3644	$\frac{1}{4}$	0.2564
O(3)	0.2265	0.2255	0.0095
O(4)	0.4249	$\frac{1}{4}$	0.1221
O(5)	$\frac{1}{2}$	0.2792	0
O(6)	0.6998	0.2222	0.1105
O(7)	0.8925	0.2926	0.2368
O(8)	0.9781	0.2686	0.1161
O(9)	0.1091	$\frac{1}{2}$	0.1970
O(10A)	0.2796	$\frac{1}{2}$	0.1250
O(10B)	0.3179	0	0.1469
O(11A)	0.5658	0	0.1252
O(11B)	0.5658	$\frac{1}{2}$	0.1252
O(12A)	0.8243	$\frac{1}{2}$	0.1089
O(12B)	0.8599	0	0.1292

features of the actual structure, the same crystal was mounted again on the CAD-4 goniometer and collection of the superstructure reflections was undertaken. Unfortunately, whatever the scanning method, all the superstructure reflections were too weak to be measured. It appeared that the crystal was too small to verify the hypothesis. Another crystal which was a plate ( $10 \times 76 \times 144 \mu\text{m}$ ) was tested and recorded in the whole space with the limits  $|h| \leq 7$ ,  $|k| \leq 7$  and  $|l| \leq 7$ . We retained the reflections which had at least three measured equivalents. Among 1790 measurements, only 7 independent reflections had a significant value. These reflections correspond precisely to the 7 highest values of  $F_c$ . This test thus confirmed the results of the structure analysis. Nevertheless, it seems that another type of superstructure exists, as suggested by the electron microscopy study which revealed also faint superstructure reflections in the  $a$  direction. This fact is perhaps related to the  $\text{Rb}^+$  distribution.

### Description of the structure and discussion

The framework of  $\text{Rb}_x\text{P}_8\text{W}_{24}\text{O}_{88}$  is built up from three-octahedra-wide perovskite slabs, connected through  $\text{P}_2\text{O}_7$  groups. As in  $\text{Rb}_x\text{P}_8\text{W}_{32}\text{O}_{112}$ , tunnels with a distorted hexagonal section running along the [010] direction occur. The location of the Rb ions in these tunnels is similar to that observed for  $n = 4$ :  $\text{Rb}^+$  is probably located on the only sites (000) which are not surrounded by two  $\text{P}_2\text{O}_7$  groups, involving for this ion an eightfold coordination with standard Rb—O distances (Table 3). Its location on the  $(0\frac{1}{2}0)$  sites, which are characterized by closely related geometry but a tenfold coordination due to the presence of the

$\text{P}_2\text{O}_7$  groups, would involve unlikely and inhomogeneous Rb—O distances. A site-potential calculation confirms this point of view; for this calculation, two extreme hypotheses were made for the charges of the atoms: (a) zero for P and O(9), (b) +5 for P and -2 for O(9), the other O atoms being -2, Rb +1 and W +5.59. In both cases the potential of the (000) site is less than the potential of the  $(0\frac{1}{2}0)$  site, by 1.1 eV in the first hypothesis and by 4 eV in the second, so that  $\text{Rb}^+$  is effectively stabilized in the (000) site at the level where  $\text{P}_2\text{O}_7$  is missing. These calculations must of course be considered only as a rough estimation due to the covalent character of the P—O bond. One notes that the O distribution of the tilted perovskite framework is enough to favour the (000) site.

In  $\text{Rb}_x\text{P}_8\text{W}_{24}\text{O}_{88}$ , both tetrahedra of the  $\text{P}_2\text{O}_7$  groups are related by symmetry, contrary to the term  $n = 4$ . Nevertheless the  $\text{P}_2\text{O}_7$  groups are almost the same in both structures, especially the P—O—P angle which is rather far from  $180^\circ$ . The P—O distances and angles are given in Table 4. P—O(9), which is the distance of P to the bridging O atom of the  $\text{P}_2\text{O}_7$  group, is the largest due to the repulsion between the P atoms. The displacement of P from the centre of its tetrahedron is  $0.07(3) \text{ \AA}$ , but does not appear in a preferential direction. In both terms  $n = 3$  and  $n = 4$ , the  $\text{P}_2\text{O}_7$  groups have the same rigid configuration, inducing in the octahedral framework some distortions and tiltings. Three types of octahedra are observed: the  $\text{W}(2)\text{O}_6$  octahedra are only linked to octahedra, while  $\text{W}(1)\text{O}_6$  and  $\text{W}(3)\text{O}_6$  share respectively one and two corners with the  $\text{PO}_4$  tetrahedra. Here,  $\text{W}(2)\text{O}_6$  is not tilted but just slightly distorted. The inclination with respect to the [010] direction is  $7.7(6)^\circ$  for the  $\text{W}(1)\text{O}_6$  octahedra and  $7.2(7)^\circ$  for  $\text{W}(3)\text{O}_6$ . These values correspond to the maximum inclination observed in the term  $n = 4$  of the series ( $7.7^\circ$ ). The deformation of the ideal perovskite framework is, however, more gradual for  $n = 4$ . The different behaviour of the term  $n = 3$  is easily

Table 3. Coordination of Rb and W atoms in the actual structure — interatomic distances ( $\text{\AA}$ )

Bond	Rb—O	W(1)—O	W(2)—O	W(3)—O
Neighbour				
O(1)	$4 \times 3.01(3)$	2.02(3)		
O(2)		1.83(3)	1.93(3)	
O(3)		2.04(3)		1.80(4)
O(4)		1.82(3)	1.93(2)	
O(5)			1.89(1)	
O(6)			2.02(4)	1.77(4)
O(7)				2.09(3)
O(8)	$4 \times 2.94(5)$			2.12(3)
O(10A)		1.91(1)		
O(10B)		1.89(1)		
O(11)			$2 \times 1.88(1)$	
O(12A)				1.88(1)
O(12B)				1.95(1)

Table 4. *The  $\text{P}_2\text{O}_7$  group in the actual structure – interatomic distances (Å) and angles (°)*

Neighbour <i>N</i>	P	O(1)	O(7)	O(8)	O(9)
P– <i>N</i>	3.10 (1)	1.57 (4)	1.53 (4)	1.43 (3)	1.60 (1)
P–O(9)– <i>N</i>	152 (2)				
O(1)–P– <i>N</i>			109 (2)	110 (2)	108 (2)
O(7)–P– <i>N</i>				113 (2)	105 (2)
O(8)–P– <i>N</i>					111 (2)

explained by the fact that the perovskite slabs are narrower than for  $n = 4$ : in the [100] direction, there is only one octahedron ensuring the connection between the octahedra which share their corners with the  $\text{P}_2\text{O}_7$  groups. It would be interesting to compare with the terms  $n > 4$  and  $n = 2$ .

The W displacement from the centre of the octahedra can also be considered. It can be seen that W(2) is not displaced [0.05 (2) Å] while the displacements of W(1) [0.14 (3) Å] and W(3) [0.22 (3) Å] are rather large, involving for W(2) an ideal octahedral coordination while W(1) and W(3) are rather (4 + 2)-coordinated as in the term  $n = 4$  (Table 3).

### Conclusion

The oxide  $\text{Rb}_x\text{P}_8\text{W}_{24}\text{O}_{88}$  is the term  $n = 3$  of the series  $\text{Rb}_x\text{P}_8\text{W}_{8n}\text{O}_{24n+16}$  previously foreseen (Giroult, Goreaud, Labbé & Raveau, 1980).

*Acta Cryst.* (1981), B37, 1166–1170

## The Structure of Yttrium Tungstate $\varepsilon\text{-Y}_2\text{WO}_6$

BY O. BEAURY, M. FAUCHER AND G. TESTE DE SAGEY

ER 210, CNRS, 92190 Meudon Bellevue, France

(Received 23 June 1980; accepted 8 December 1980)

### Abstract

The high-temperature polymorph  $\varepsilon\text{-Y}_2\text{WO}_6$  is orthorhombic, space group  $P2_12_12_1$ , with  $a = 8.591$  (5),  $b = 20.840$  (10),  $c = 5.233$  (5) Å,  $Z = 8$ ,  $D_m = 6.38$ ,  $D_c = 6.49$  Mg m<sup>-3</sup>. The structure was determined at room temperature from 454 diffractometer intensities and refined to  $R = 0.067$ . The W atoms are octahedrally coordinated and far apart from each other. The four non-equivalent Y atoms have an eightfold (3) and sevenfold (1) coordination number. Reference is made to the fluorescence spectrum of the Eu-doped compound and a comparison is made with the homologous compounds  $\text{Ln}_2\text{WO}_6$  (Ln = La to Lu).

0567-7408/81/061166-05\$01.00

### References

The structural study of this term confirms the ability of the  $\text{P}_2\text{O}_7$  group to accommodate an octahedral framework such as that of perovskite in spite of its rigidity. The latter, however, undergoes deformations by tilting of its octahedra.

The comparison of both structures  $n = 3$  and  $n = 4$  shows that the cages and tunnels with a distorted hexagonal section running along [010] are similar. The location of  $\text{Rb}^+$  in eightfold sites, at the level where the  $\text{P}_2\text{O}_7$  groups are missing, is a common character to both structures confirmed here by site-potential calculations. The evolution of the deformation of the octahedral framework, different in both structures, agrees with the different widths of the perovskite slabs.

The mixed valence of W allows us to expect, for this oxide, electrical properties which could be correlated to those of perovskite bronze,  $\text{Na}_x\text{WO}_3$ , but an anisotropic character should be observed.

CROMER, D. T. (1965). *Acta Cryst.* **18**, 17–23.

CROMER, D. T. & WABER, J. T. (1965). *Acta Cryst.* **18**, 104–109.

GIROULT, J. P., GOREAUD, M., LABBÉ, PH. & RAVEAU, B. (1980). *Acta Cryst.* **B36**, 2570–2575.

SUZUKI, T. (1960). *Acta Cryst.* **13**, 279.

### Introduction

Few structure determinations have been carried out on the mixed oxides of W and trivalent rare-earth elements and Y (Bevan & Summerville, 1979). However, their relationship with scheelite suggests efficient luminescent properties and this has stimulated interest for U-activated  $\text{Y}_2\text{WO}_6$ ,  $\text{U}^{6+}$  in particular (Blasse, Van den Heuvel & Van Hesteren, 1977). Doubtless, more knowledge of the structural features of tungstates would help in the interpretation of their optical spectra and mechanisms of site-to-site energy transfer.

The rare-earth tungstates with the composition  $\text{Ln}_2\text{WO}_6$  previously investigated fall into three struc-

© 1981 International Union of Crystallography